Sustainable Cities and Society 28 (2017) 30–41

Contents lists available at ScienceDirect

Sustainable Cities and Society

journal homepage: www.elsevier.com/locate/scs

Factors governing mass transfer during membrane electrodialysis regeneration of LiCl solution for liquid desiccant dehumidification systems

Ali Al-Jubainawi [a], Zhenjun Ma [a,*], Yi Guo [a], Long D. Nghiem [b], Paul Cooper [a], Weihua Li [c]

[a] Sustainable Buildings Research Centre, University of Wollongong, NSW, 2522, Australia
[b] School of Civil, Mining & Environmental Engineering, University of Wollongong, NSW, 2522, Australia
[c] School of Mechanical, Materials & Mechatronic Engineering, University of Wollongong, NSW, 2522, Australia

ARTICLE INFO

Article history:
Received 19 May 2016
Received in revised form 21 August 2016
Accepted 25 August 2016
Available online 26 August 2016

Keywords:
Liquid desiccant
Mass transfer
Electrodialysis
Experimental investigation
Numerical simulation

ABSTRACT

This study investigates the mass transfer mechanisms and the performance of membrane electrodialysis (ED) for regenerating lithium chloride (LiCl) solution commonly used in liquid desiccant dehumidification systems. Experiments were conducted using an ED experimental system while numerical simulation was performed using COMSOL Multiphysics. The results showed that the water flux transfer due to osmosis and electro-osmosis during ED regeneration of LiCl liquid desiccant was significant and could not be ignored. The water flux due to osmosis and electro-osmosis is directly associated with the osmotic gradient and the applied current between the cathode and anode, respectively. The average flux of water from the spent solution to the regenerated solution decreased from 0.292 to 0.161 g/s m^2 when the initial concentration of the solutions in the spent and regenerated tanks increased from 18 to 30% (wt/wt) with the same applied current of 12 A and the same solution flow rate of 100 L/h. On the other hand, the salt flux due to osmosis was insignificant. The average salt flux transfer was 0.0053 g/s m^2 when the initial concentration difference between the regenerated and the spent channels was 25% (wt/wt). Simulations were conducted to elucidate the relationship between the concentration profile of LiCl solution along the membrane surface and the concentration polarization in the ED channel with respect to the circulation flow rate and applied current. Overall, the results suggest that the concentration difference between the regenerated and spent LiCl solutions should be minimized for an optimum ED performance.

1. Introduction

The increase in energy demand for air conditioning and climate changes are some of the most significant challenges facing the building sector (Pérez-Lombard, Ortiz, & Pout, 2008). The building sector accounts for around 40% of total world energy usage, of which about 50% is attributed to heating, ventilation and air-conditioning (HVAC) systems (Duan et al., 2012; Lin, Ma, Sohel, & Cooper, 2014). Building energy efficiency is therefore essential to reduce global energy usage and greenhouse gas emissions.

Over the last few decades, many energy efficient technologies have been proposed for improving the performance of building HVAC systems (Chua, Chou, Yang, & Yan, 2013; Marszal et al., 2011; Wang, Ma, & Gao, 2010). Among them, desiccant cooling has emerged as an attractive approach (Daou, Wang, & Xia, 2006; Niu, Xiao, & Ma, 2012). Desiccants are hygroscopic or dehumidified substances with the ability to attract moisture from air based on their affinity to water (Daou et al., 2006; Waugaman, Kini, & Kettleborough, 1993). To maintain the dehumidification capability, it is necessary to continuously regenerate the desiccant to remove water molecules from the system (Mohammad, Mat, Sulaiman, Sopian, & Al-abidi, 2013).

Regeneration of liquid desiccants is therefore a key process in a desiccant dehumidification system. Solar thermal regeneration has been commonly considered since solar energy availability usually coincides with the high demand of building cooling demand (Misha, Mat, Ruslan, & Sopian, 2012). Nevertheless, the high temperature of liquid desiccants after the regeneration process can impede the overall performance of desiccant dehumidification systems. Therefore, several non-thermal regeneration techniques have also been studied. Al-Sulaiman, Gandhidasan, & Zubair (2007) proposed a liquid desiccant cooling system using a reverse osmosis (RO) process

* Corresponding author.
E-mail addresses: zhenjun@uow.edu.au, mzjxjtu@163.com (Z. Ma).

http://dx.doi.org/10.1016/j.scs.2016.08.021
2210-6707/

Nomenclature

A	Membrane surface area (m^2)
B	Membrane water permeability ($mol.m^{-2}\,s^{-1}\,bar^{-1}$)
C	Weight per weight concentration (% (wt/wt))
c	Molar concentration ($mol\,m^{-3}$)
D	Diffusion coefficient ($m^2\,s^{-1}$)
F	Faraday's constant ($96485C\,mol^{-1}$)
i	Current density ($A\,m^{-2}$)
J	Molar flux ($mol\,s^{-1}\,m^{-2}$) or mass flux ($g\,s^{-1}\,m^{-2}$)
m	Number of the independently measured variables
N	Number of cells
n	Mole number
R	Gas constant ($m^3 bar\,K^{-1}\,mol^{-1}$)
T	Temperature (K)
t	Time (s)
t_w	Water transport number
u	Ions mobility ($s\,mol\,kg^{-1}$)
V	Volume (m^3)
$\dot{V}$	Volumetric flow rate ($m^3\,s^{-1}$)
v	Velocity ($m\,s^{-1}$)
x	Independently measured variable
y	Calculated variable
z	Charge number of ions

Greek symbol

ρ	Solution density ($g\,m^{-3}$)
ϕ	Solution potential (volt)
π	Osmotic pressure (bar)

Superscript

j	Initial condition
t	Time (s)

Subscript

Dif	Diffusion
eos	Electro-osmosis
G	Regenerated
GT	Regenerated tank
in	Inlet
I	Applied current
M	Membrane
os	Osmosis
S	Spent
ST	Spent tank
s	Species in solution
tot	Total
w	Water

for desiccant regeneration. However, a pump with high pressure was required to overcome the high osmotic pressure of the liquid desiccant. Another approach is to use an electrodialysis (ED) process to regenerate liquid desiccants (Li & Zhang, 2009). ED is an ion-exchange membrane separation process. In ED, ions can be transported through selective cation or anion membranes under an electric potential gradient (Strathmann, 2004). Owing to the selectivity of ion-exchange membranes, cations and anions can only migrate through cation-exchange membranes (CEMs) and anion-exchange membranes (AEMs), respectively.

The use of ED for liquid desiccant regeneration was first proposed by (Li & Zhang, 2009), who used a single stage photovoltaic-electrodialysis (PV-ED) system. A double stage PV-ED system was subsequently developed by Li, Zhang, & Quan (2011), leading to 50% energy savings in comparison to their first single stage PV-ED system. Cheng, Zhang, & Li (2013) further developed a hybrid ED regeneration system, in which the heat generated by solar photovoltaic thermal collectors was used to pre-treat the liquid desiccant solution before entering the ED stack. The results from these studies have demonstrated the potential practicality of ED technology for liquid desiccant regeneration. However, the remaining technical challenge is to determine the operating envelope and optimize ED operation specifically for liquid desiccant regeneration.

Mass transfer of ions and water in ion-exchange membranes has been extensively investigated both theoretically and experimentally (Casas, Aladjem, Cortina, Larrotcha, & Cremades, 2012; Casas et al., 2011; Fidaleo & Moresi, 2005; Nikonenko, Lebedev, Manzanares, & Pourcelly, 2003; Ortiz et al., 2005; Sadrzadeh, Kaviani, & Mohammadi, 2007; Tanaka, 2003, 2006; Zourmand, Faridirad, Kasiri, & Mohammadi, 2015). However, most previous studies were in the context of sea or brackish water desalination in which salt concentrations in the feed were much lower than that in liquid desiccant regeneration. Tanaka (2003) developed an experimental and theoretical procedure to investigate the mass transport and energy consumption of ED for seawater desalination. Nikonenko et al. (2003) developed a model which considered two chemical species in the external diffusion boundary. The mechanism of the competitive transport of anions through AEMs was described using Nernst-Plank and Donnan equations (Nikonenko et al., 2003). A mathematical model based on Nernst-Plank equation was also used by Casas et al. (2012); Casas et al. (2011) to predict the performance of an ED system for concentrating the brine of the reverse osmosis of the seawater desalination process.

To date, there have been very few attempts to experimentally examine the performance of ED specifically for liquid desiccant regeneration. An experimental setup was developed by Cheng, Xu, & Zhang (2013) to examine the effect of the solution flow rate on the mass transfer and current utilization of the ED stack. Guo, Ma, Al-Jubainawi, Cooper, & Nghiem (2016) experimentally investigated the effects of four operating parameters of ED on the concentration increase of the lithium chloride (LiCl) liquid desiccant solution. The four operating parameters considered were the initial concentration of the regenerated solution, the initial concentration difference between the regenerated and spent solutions, the applied current density and the solution flow rate. The results from the experimental tests showed that ED technology can be potentially useful for liquid desiccant regeneration if the operating conditions of ED are properly selected. However, the mechanisms governing the mass transfer inside the ED stack for liquid desiccant regeneration have not been examined.

A key distinction between ED for desalination and liquid desiccant regeneration is the mass transfer induced by osmotic, electro-osmotic, ion migration, and diffusion. This study aims to elucidate the mass transfer mechanisms of ED for regenerating LiCl liquid desiccant commonly used in desiccant cooling systems. The originality of this work is to employ a combination of both numerical simulation and experimental evaluation to examine the behaviors and concentration profile of the ED stack under different operating conditions to understand the fundamental mechanisms governing the mass transfer of the ED for liquid desiccant regeneration.

2. Theory and research methods

2.1. Mass transfer mechanisms

There are four major mass transfer mechanisms in ED, namely electro-osmosis, osmosis, ion migration and diffusion. Electro-osmosis and osmosis are responsible for water transport. Ion

migration and diffusion govern the ions transport through the membrane. Osmosis occurs when there is a concentration difference between the spent and regenerated solutions across the membrane. Osmosis leads to the transfer of water from the spent solution (low osmotic pressure) to the regenerated solution (high osmotic pressure) and the salt diffusion in the opposite direction (Strathmann, 2004). Salt diffusion through selective membranes is generally small compared to that governed by ion migration, which is induced by an applied electric potential between the cathode and anode of the ED stack (Tanaka, 2010; Zourmand et al., 2015). Because of hydration, each ion in an aqueous solution is surrounded by a thin layer of water molecules (Strathmann, 2004). These water molecules will transport together with the migrated ions due to the electro-osmosis phenomena (Tanaka, 2010). Thus, the concentration and the volume of the regenerated solution increase due to the ions migration and water transfer when an electric current is applied to the ED stack.

2.2. Outline of the research and data analysis method

The research method used to investigate the mass transfer mechanisms of ED for liquid desiccant regeneration is illustrated in Fig. 1. It mainly consists of three steps: i) the experimental design and experimental tests; ii) the ED characteristics identification, and the modelling system setup and validation; and iii) the experimental and numerical investigation of the mass transfer mechanisms of ED for liquid desiccant regeneration.

A range of experimental tests, as summarized in Table 1, were first designed and conducted based on a lab-scale ED experimental setup, which will be introduced in Section 3. Based on the experimental data collected, the ED characteristics such as the membrane water permeability and the water transport number were then identified and used to set up the numerical model. The experimental data was also employed to validate the effectiveness of the numerical model used. Lastly, the experimental data is used to investigate the salt transfer due to the applied electric current and diffusion, and the water transfer due to the different osmotic pressures and the electro-osmosis impact. In the meanwhile, the validated numerical model is used to investigate the concentration profiles of the liquid desiccant within the ED stack, boundary layer distribution, and Li^+ ions moving through the CEMs and Cl^- ions moving through the AEMs, as well as the concentrations of the solutions at the exit of the ED stack.

The water flux ($J_{w,os}$) and salt flux ($J_{salt,Dif}$) through the ED channels due to osmosis and diffusion without current apply can be determined using Eqs. (1) and (2), respectively. When an electric current is applied, both osmosis and electro-osmosis can affect the water flux from the spent channels to the regenerated channels and the total water flux ($J_{w,tot}$) transferred can be determined by Eq. (3).

The net salt mass flux ($J_{salt,net}$) through the ED membranes with an applied current is a combination of the effects of the ions migration and diffusion, and can be calculated by Eq. (4). The mass flux from the spent channels to the regenerated channels of the ED stack (J_{ED}) can therefore be determined by Eq. (5).

$$J_{w,os}^{j+t} = \frac{1}{2N.A.t}\left[\rho_{GT}^{j+t}V_{GT}^{j+t}\left(1-C_{GT}^{j+t}\right)-\rho_{GT}^{j}V_{GT}^{j}\left(1-C_{GT}^{j}\right)\right] \quad (1)$$

$$J_{salt,Dif}^{j+t} = \frac{1}{2N.A.t}\left[\rho_{ST}^{j+t}V_{ST}^{j+t}C_{ST}^{j+t}-\rho_{ST}^{j}V_{ST}^{j}C_{ST}^{j}\right] \quad (2)$$

$$J_{w,tot}^{j+t} = J_{w,os}^{j+t}+J_{w,eos}^{j+t} = \frac{1}{2N.A.t}\cdot\left[\rho_{GT}^{j+t}V_{GT}^{j+t}\left(1-C_{GT}^{j+t}\right)-\rho_{GT}^{j}V_{GT}^{j}\left(1-C_{GT}^{j}\right)\right] \quad (3)$$

$$J_{salt,net}^{j+t} = J_{salt,I}^{j+t}-J_{salt,Dif}^{j+t} = \frac{1}{2N.A.t}\left[\rho_{GT}^{j+t}V_{GT}^{j+t}C_{GT}^{j+t}-\rho_{GT}^{j}V_{GT}^{j}C_{GT}^{j}\right] \quad (4)$$

$$J_{ED}^{j+t} = J_{w,tot}^{j+t}+J_{salt,net}^{j+t} \quad (5)$$

where $J_{salt,I}$ and $J_{w,eos}$ are respectively the salt flux and water flux due to applied current, and C, ρ, t, N, A and V are the concentration, density, operating time, cell number, effective membrane area and volume of the solution respectively, the superscripts $j+t$ and j represent the time since the start of the test and the start time of the test respectively, and the subscripts GT and ST indicate the regenerated and spent tanks, respectively.

The concentration of the solution transferred from the spent channels to the regenerated channels (C_{ED}) can be determined by Eq. (6), which can provide an indication of the ED regeneration performance under different operating conditions.

$$C_{ED}^{j+t} = \frac{J_{salt,net}^{j+t}}{J_{w,tot}^{j+t}+J_{salt,net}^{j+t}} \quad (6)$$

Because of ion and water transport, the concentration and volume in both regenerated and spent tanks vary with time. These changes can be calculated using the mass balance equation for both spent and regenerated tanks. Therefore, the concentrations of the spent and regenerated solutions at the exit of the ED stack can be determined by Eqs. (7) and (8), respectively.

$$C_{G,exit}^{j+t} = \frac{C_{GT}^{j+t}.\rho_{GT}^{j+t}.\dot{V}_1+2N.A.(J_{ED}^{j+t}.C_{ED}^{j+t})}{\rho_{GT}^{j+t}.\dot{V}_1+2N.A.J_{ED}^{j+t}} \quad (7)$$

$$C_{S,exit}^{j+t} = \frac{C_{ST}^{j+t}.\rho_{ST}^{j+t}.\dot{V}_2-2N.A.(J_{ED}^{j+t}.C_{ED}^{j+t})}{\rho_{ST}^{j+t}.\dot{V}_2-2N.A.J_{ED}^{j+t}} \quad (8)$$

where $C_{G,exit}$ and $C_{S,exit}$ are the concentrations of the solutions at the exits of the regenerated channels and spent channels respectively, and $\dot{V}_1$ and $\dot{V}_2$ are the volumetric flow rates of the inlet solutions into the regenerated and spent channels, respectively.

2.3. Numerical modelling of the ED cell

An ED cell consisting of one regenerated domain, two spent domains, and one pair of cation and anion exchange membranes was modelled in this study (Fig. A1 in Appendix A). The geometric dimensions of the ED cell were specified based on the manufacturing data of the experimental setup to be introduced in Section 3. The key parameters used in the model are summarized in Table B1 in Appendix B.

Nernst-Plank equation has been extensively used to simulate the ions transport through ED membranes (Casas et al., 2011; Fadaei, Shirazian, & Ashrafizadeh, 2011; Tanaka, 2010; Zourmand et al., 2015) and this equation has been included in the electrochemistry component of COMSOL Multiphysics Software. COMSOL Multiphysics is a commercial finite element package designed to address a wide range of physical phenomena (Dickinson, Ekström, & Fontes, 2014). The procedures used to simulate ED for liquid desiccant regeneration using COMSOL Multiphysics are similar to those presented in (Bawornruttanaboonya, Devahastin, Yoovidhya, & Chindapan, 2015; Zourmand et al., 2015).

Nernst-Plank equation for the diffusion, migration and convection to simulate the ions movement behavior inside the ED cells is shown in Eq. (9).

$$J_s = -D_s\nabla c_s - z_s u_s F c_s \nabla\phi + c_s v \quad (9)$$

where J and c stand for the molar flux and the concentration respectively, D is the diffusion coefficient of species, z is the charge number of ions, u is the mobility, F is the Faraday constant, ϕ is the solution

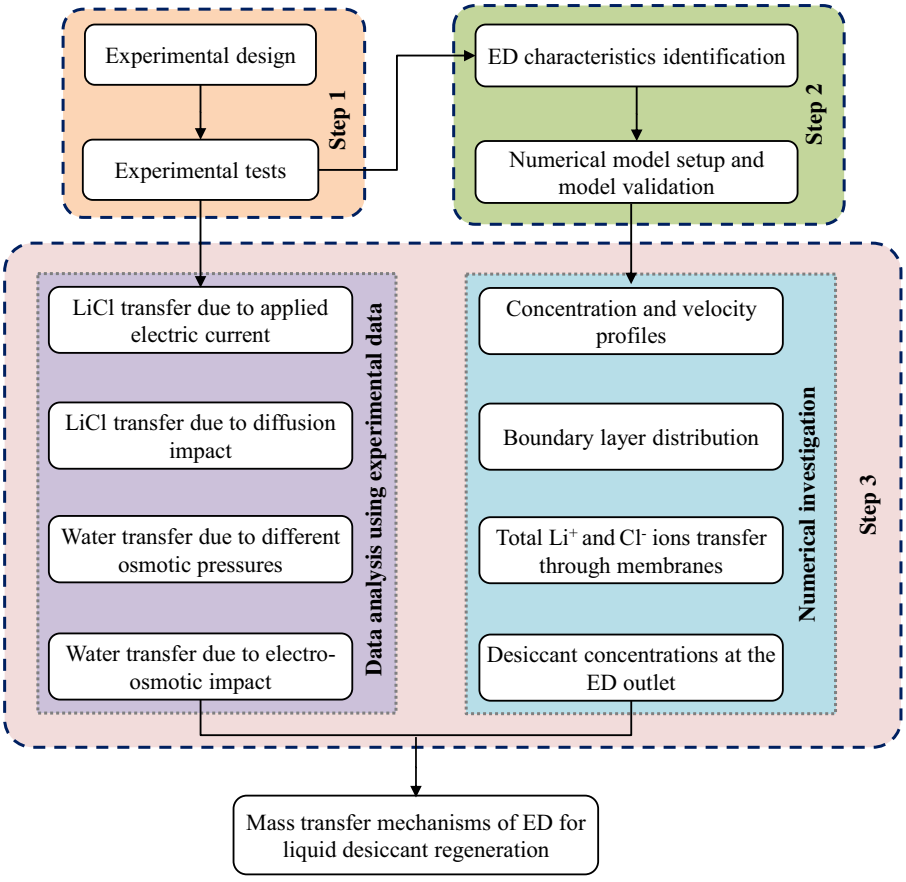

Fig. 1. Method employed to investigate the mass transfer mechanisms of the ED for liquid desiccant regeneration.

Table 1
Designed experiments for investigating the characteristics of the ED for liquid desiccant regeneration.

Cases	Description	Factors				
		C_{GT} (%(wt/wt))	C_{ST} (%(wt/wt))	Flow rate (L/h)	Current (A)	Operating time (hour)
1	Osmotic pressure, water flux transfer and salt flux transfer	30	25	100	0	2
2		30	20	100	0	2
3		30	15	100	0	2
4		30	10	100	0	2
5		30	5	100	0	2
6	Electro-osmotic force, and salt and water mass transfer	30	30	100	3–12	2
7		27.5	27.5	100	3–12	2
8		25	25	100	3–12	2
9		18	18	100	3–12	2
10	Combined effects of the variables designed using an orthogonal layout with 4 factors and 3 levels	29	29	60	8	1
11		29	27.5	100	10	1
12		29	26	140	12	1
13		27.5	27.5	140	10	1
14		27.5	26	60	12	1
15		27.5	24.5	100	8	1
16		26	26	100	12	1
17		26	24.5	140	8	1
18		26	23	60	10	1
19	Impact of solution flow rate on the ED exit concentration	27.71	27.71	60	8	2
20		27.71	27.71	100	8	2
21		27.77	27.20	140	8	2

potential, v is the fluid velocity vector, and the subscript s represents the kind of species such as cations and anions.

For liquid desiccant regeneration, the product from the ED stack is the regenerated solution with a high concentration and the performance of the ED regeneration can be affected by the amount of water transferred from the spent channels to the regenerated channels. The molar flux of water through the selective membranes due to the osmosis can be calculated by Eq. (10) (Holloway, Childress, Dennett, & Cath, 2007; Zhao & Zou, 2011). The osmotic pressure in the regenerated and the spent solutions is determined by Eq. (11) (Amjad, 1993; Zhao & Zou, 2011). The water molar flux due to electro-osmosis can be calculated by using Eq. (12) (Tanaka, 2010),

in which the water transport number due to the electro-osmosis and the water permeability factor of the membranes due to osmosis were obtained from the experiments (i.e. Experimental cases 1–9 in Table 1).

$$J_{w,os} = B(\pi_G - \pi_S) \quad (10)$$

$$\pi = nRTc \quad (11)$$

$$J_{w,eos} = \frac{t_w i}{F} \quad (12)$$

where B is the water permeability factor of AEMs and CEMs which is calculated based on overall water transfer from the low concentration side to the high concentration side of the membrane wall, π is the osmotic pressure, c is the molar concentration of the solution, n is the moles number of the solute in the solution (e.g. n = 2 for LiCl), R is the gas constant, T is the absolute solution temperature, i is the applied current density, t_w is the water transport number of membranes, and the subscripts G and S represent the regenerated and spent channels, respectively.

The heat transfer between the spent and regenerated channels of the ED cells was not considered in this study. In addition, it was assumed that the regenerated and spent channels have the same hydrodynamic characteristics as the same solution flow rates were used in both flow channels.

The major boundary conditions used for modelling of the ED stack for liquid desiccant regeneration were similar to those presented by Zourmand et al. (2015) and they are briefly summarized below.

- The potential drop across the ED cell is constant;
- The concentrations of the spent and regenerated solutions at the ED entrance are uniform;
- The gradient diffusion flux at the exit of the ED channels equals to zero; and
- The current density of the solution equals to the current density of the membrane.

3. Materials and methods

3.1. Electrodialysis experimental system

A lab-scale ED system (Fig. A2 in Appendix A) consisting of an ED stack, a rectifier (PowerTech MP3090) and a power transformer was used. The key specifications of the ED stack (Asahi Glass Corp., Tokyo, Japan) are summarized in Table B1 in Appendix B. Lithium sulfate (Li_2SO_4) solution was used as the electrode rinsing solution in the ED stack. Two extra cation CMV membranes were used at the cathode and anode to prevent sulfate from migrating into the spent and regenerated solutions. The regenerated, spent and rinsing electrolyte solutions were circulated through three 3.5 L transparent PVC tanks, respectively. The solutions were circulated through the ED stack by three magnetic drive pumps. Further details of this ED system are available elsewhere (Guo et al., 2016).

A portable density meter (30PX Densito) was used to measure the density and temperature of the aqueous LiCl solutions in both regenerated and spent tanks. The measured density and temperature were then used to calculate the concentrations of the LiCl solutions. Three direct indication type variable area flow meters with a scale range of 60–600 L/h were used to measure the solution flow rate in each individual flow stream.

The uncertainties related to the experiments include the uncertainty of the measured variables and the uncertainty of the calculated variables. The measured variables include the density, the temperature and the volume of the solutions. The calculated variables include the water mass transfer due to osmosis and electro-osmosis, and the net salt mass transfer due to the diffusion and ions migration.

The basic root-sum-square method can be used to determine the relative uncertainty of the calculated variables (Yang, Sun, & Chen, 2015). The relative uncertainty for a calculated variable y with a set of independently measured variables x_i can be determined by Eq. (13). Based on Eq. (13), it was determined that the maximum composite relative uncertainties for the calculated water mass transfer and salt mass transfer of the liquid desiccant in all experiments were 3.5 and 10.6%, respectively. The major measuring instruments used and their claimed measurement accuracies are summarized in Table B2 in Appendix B.

$$\frac{\delta y}{y} = \frac{\sqrt{\sum_m^{i=1}\left(\frac{\partial y}{\partial x_i}\partial x_i\right)^2}}{y} \quad (13)$$

where m is the number of the independently measured variables.

3.2. Experimental protocol

Four sets of the experiments (Table 1) were designed to investigate the mass transfer mechanisms and the impact of the solution flow rate and the applied current on the performance of ED for liquid desiccant regeneration. The density and temperature of the solutions in both spent and regenerated tanks were measured every 5 min. The variation in the volume levels in both regenerated and the spent solution tanks was also observed and recorded every 5 min. During the experiments, the solution flow rates were manually controlled by a globe valve. All the experiments were carried out under the room temperature conditions. The majority of the experiments were also duplicated to increase the reliability of the experiments.

The first experimental set was designed to examine the water transfer through the membranes resulting from the osmotic pressure difference between the spent and regenerated channels, and investigate the salt transfer from the regenerated channels to the spent channels due to diffusion. The second experimental set investigated the water transfer through the selective membranes due to the electro-osmotic impact when different currents were applied to the ED stack. The third experimental set was designed using an orthogonal layout with 4 factors and 3 levels. This set of experiments was to examine the salt mass transfer through the membranes with different combinations among the applied electric current, solution flow rate, and the initial concentrations of the solutions in the spent and regenerated tanks. It is worthwhile to mention that, for this group of experiments, the duration of each experiment was one hour as the major purpose is to investigate the combined effect of the variables considered. The last experimental set was designed to examine the effects of the solution flow rate on the performance of the ED for liquid desiccant regeneration.

4. Results and discussions

4.1. Model validation

To ensure the Nernst-Plank model validity for liquid desiccant regeneration, the results obtained using COMSOL Multiphysics were validated using the data collected from the third experimental set (Fig. 2). The simulated concentration difference of the solution at the entrance and exit of the regenerated channels was in a good agreement with that derived from the experimental data. The results in Fig. 2 confirmed that the Nernst-Plank model integrated in COMSOL Multiphysics can provide acceptable estimates for predicting the concentration of the solution at the ED outlet.

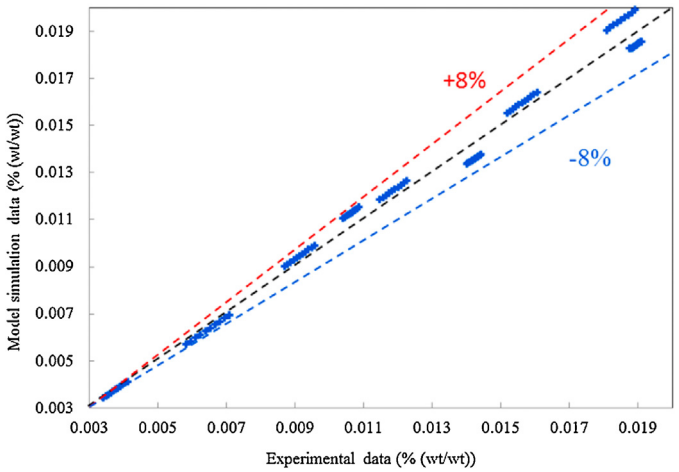

Fig. 2. Comparison between the model simulated concentration difference between the entrance and exit of the ED stack and that derived from the experimental data.

4.2. Water and salt transfer due to osmosis

Fig. 3 shows the osmotic pressure differences between the spent and regenerated channels, and the fluxes of water and LiCl through the membranes at various concentration differences between the two solutions (i.e. Experimental cases 1–5). There was no electric potential between the cathode and anode in order to eliminate any electro-osmosis effect.

The osmotic pressure difference between the spent and regenerated channels decreased with operating time since the concentration difference between both channels decreased continuously over time (Fig. 3a). As shown in Fig. 3b, the average water flux from the spent to the regenerated solutions within 2 h operation was about 0.23 g/s m^2 when the initial concentration difference between the regenerated and spent solutions was 25% (wt/wt), whereas the average water flux decreased to 0.026 g/s m^2 when the initial concentration difference between the regenerated and spent solutions decreased to 5% (wt/wt). For this group of the experiments, the maximum increase of the regenerated and spent solution temperature during the 2 h test was 3.9 °C. This temperature increase is mainly due to the heat rejection from the solution pumps and the variation in the room temperature.

Salt flux transfer due to the concentration difference between the regenerated and spent solutions was generally small when comparing to that of water flux transfer (Fig. 3c). The average salt flux transfer was 0.0053 g/s m^2 when the initial concentration difference between the regenerated and the spent solutions was 25% (wt/wt).

Overall, water transfer due to osmosis is more significant than salt transfer. It is therefore necessary to minimize the concentration difference between the regenerated and spent solutions to control the negative impact of osmosis on the ED performance for liquid desiccant regeneration.

4.3. Water transfer due to electro-osmosis

In this study, four experiments (i.e. Experimental cases of 6–9) were carried out to investigate the impact of the electro-osmosis on the amount of water mass transfer from the spent channels to the regenerated channels. The initial concentrations of the spent and regenerated solutions were identical to avoid any osmosis effect.

Fig. 4 shows the water mass transfer from the spent to the regenerated channels under different applied currents. The flux of water transfer increased with the increase of the applied current. When the initial concentrations of the solutions in both spent and regenerated tanks were 30% (wt/wt) and the solution flow rate of 100 L/h, the average flux of water transfer was about 0.161 and 0.035 g/s m^2 when the applied currents were 12 and 3 A, respectively (Fig. 4a). The maximum increase of the solution temperature during the 2 h test was 1.8 °C when the applied current was 3 A while that was 4.5 °C when the applied current was 12 A. This temperature increase was probably resulted from the heat rejection from the solution pumps and the heat generated because of the Joule effect as well as the variation in the room temperature.

When the initial concentration of the solutions in both spent and regenerated tanks was 18% (wt/wt), the average flux of water from the spent channels to the regenerated channels increased to 0.292 and 0.073 g/s m^2 when the applied currents were 12 and 3 A, respectively (Fig. 4b). The flux of water through the membranes

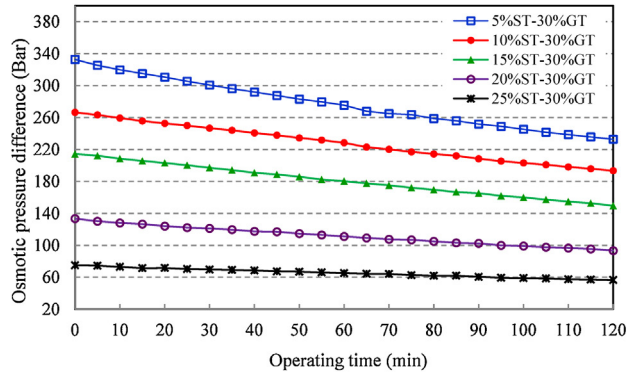

(a) Osmotic pressure difference between spent and regenerated channels

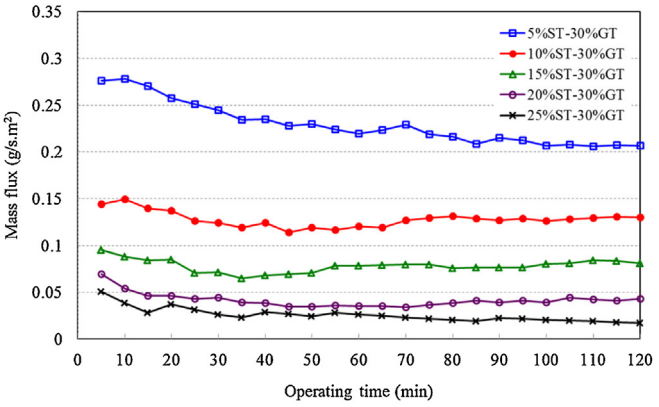

(b) Water flux transfer from the spent to regenerated channels

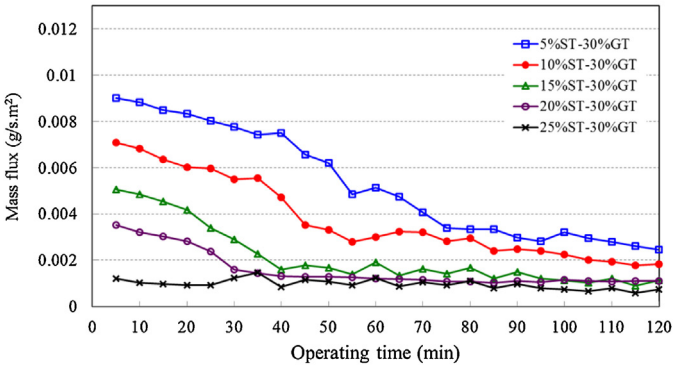

(c) Salt flux transfer from the regenerated to spent channels

Fig. 3. Impact of different initial concentrations of the solutions in the regenerated and spent tanks on the water/salt flux transfer through the ED stack, where ST and GT represent the spent tank and regenerated tank, respectively.

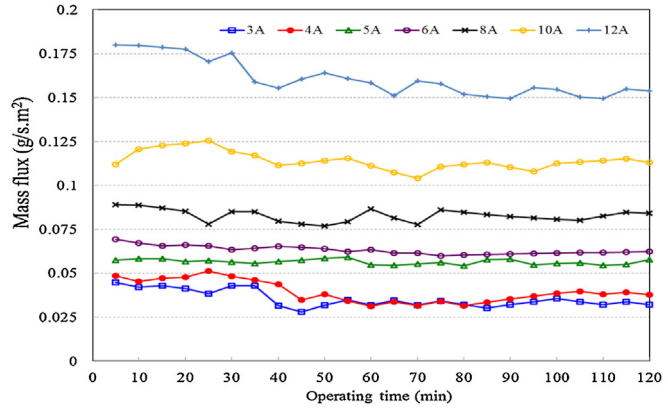

(a) Initial solution concentrations of 30% (wt/wt)

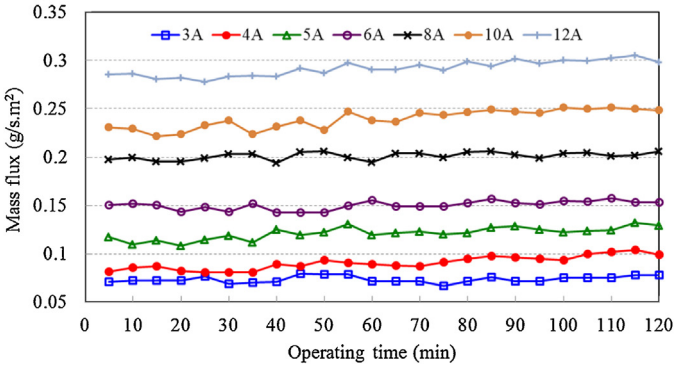

(b) Initial solution concentrations of 18% (wt/wt)

Fig. 4. Water mass transfer from the spent to regenerated channels due to the impact of electro-osmosis.

Table 2
Salt flux transfer within the ED under different operating conditions.

Cases	C_{GT} (%(wt/wt))	C_{ST} (%(wt/wt))	Flow rate (L/h)	Current (A)	Salt flux (g/s m^2)	$\overline{\Delta C}$% (wt/wt)
10	29	29	60	8	0.048	0.01578
11	29	27.5	100	10	0.062	0.00847
12	29	26	140	12	0.079	0.00547
13	27.5	27.5	140	10	0.065	0.01008
14	27.5	26	60	12	0.079	0.01814
15	27.5	24.5	100	8	0.053	0.0032
16	26	26	100	12	0.082	0.01885
17	26	24.5	140	8	0.054	0.00655
18	26	23	60	10	0.071	0.01099

decreased with increasing initial concentration of the solutions in the spent and regenerated tanks. This phenomenon was resulted from high water activity in the low solution concentration as well as the obstruction of the boundary layers for mass transfer through ion exchange membranes, where an increased solution concentration led to an increased solution viscosity thereby increasing the boundary layer thickness at the membrane walls (Kim, 2010).

4.4. Ion transfer due to applied current

The salt flux transfer during ED regeneration was analyzed using the third experiment set (i.e. Experiments cases 10–18). Table 2 summarizes the salt flux from the spent to the regenerated channels within one hour test under different operating conditions. Salt flux transfer can be generally classified into three groups of 0.048–0.054, 0.062–0.071 and 0.079–0.082 g/s m^2 corresponding to the applied currents of 8, 10 and 12 A, respectively. The applied current is the most influential parameter for the salt flux through

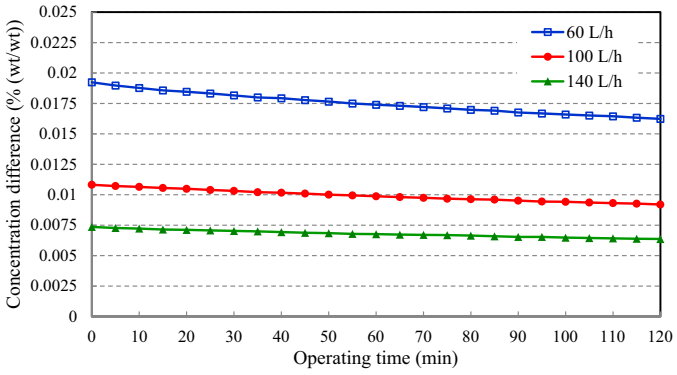

Fig. 5. Variation of the concentration difference of the regenerated solution between the inlet and outlet of the ED stack under different solution flow rates (initial concentrations of the solutions in regenerated and spent tanks of 27.71% (wt/wt) and the applied current of 8 A).

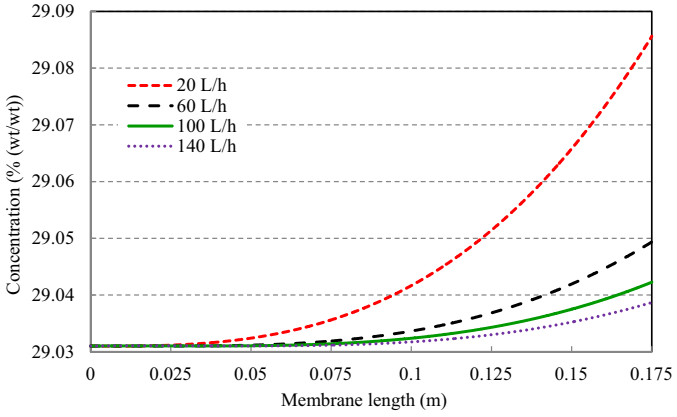

Fig. 6. Concentration of the regenerated solution along the membrane length under different solution flow rates.

the membranes. Increasing the applied current increased the salt flux from the spent to the regenerated channels regardless of the solution flow rate and the initial concentrations of the solutions in both spent and regenerated tanks.

The average concentration difference of the regenerated solution between the entrance and the exit of the ED stack ($\overline{\Delta C}$) during the whole test period for each case is also shown in Table 2. However, it is hard to identify which factor has a higher impact on the ED regeneration performance. Basically, the regeneration performance is related to the salt mass transfer from the spent channels to the regenerated channels and this salt mass transfer is directly associated with the applied current.

The impact of the solution flow rate on the ED regeneration performance was investigated based on the experimental data from the experimental cases of 19–21 (Fig. 5). As expected, the concentration difference of LiCl desiccant solution between the inlet and outlet of the ED stack increased with decreasing solution flow rate due to the increase of the residence time of the solution inside the ED stack.

Current efficiency, which is a fraction of the electric charge transported by ions in the total amount of electric charge applied to the ED cell (Wang, Xing, Jia, & Ren, 2015) can be used to evaluate the energy performance of the ED. The use of current efficiency to analyze the performance of ED for liquid desiccant regeneration can be found in Guo et al. (2016).

4.5. Concentration profile of LiCl in the ED channels

The concentration profiles of LiCl along the ED cell with different solution flow rates were simulated under the applied current

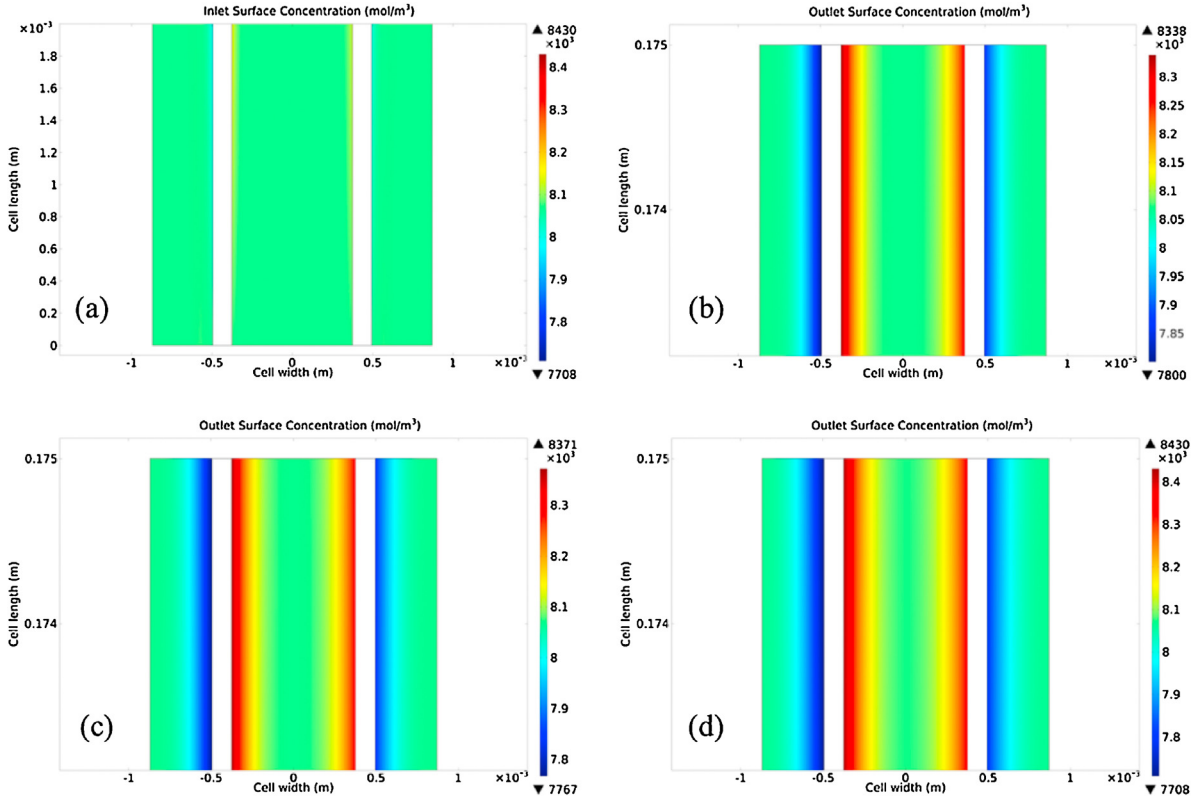

Fig. 7. Concentration distributions of the solution at the inlet and outlet of the ED cell a) inlet; b) outlet at 140 L/h; c) outlet at 100 L/h; d) outlet at 60 L/h.

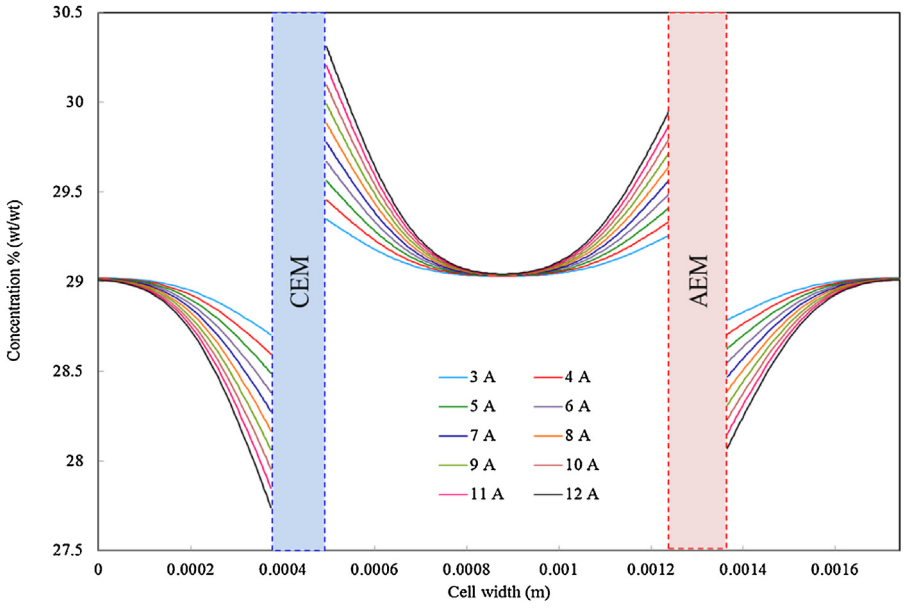

Fig. 8. Concentration distribution of the solution through the ED cell and along the membranes under different applied currents.

of 8 A and the initial concentrations of both spent and regenerated solutions of 29.031% (wt/wt) and the results are presented in Fig. 6. The concentration of the regenerated solution continuously increased along the length of the membranes and the concentration of the solution at the ED outlet increased with the decrease of the solution flow rate. The concentration difference of the solution between the inlet and outlet of the regenerated channel was 0.053% (wt/wt) when the membrane length was 0.175 m and the solution flow rate was 20 L/h. The concentration difference of the solution between the inlet and outlet of the regenerated channel decreased to 0.0077% (wt/wt) when the solution flow rate was increased to 140 L/h while keeping the other operating conditions were the same. The above results showed that decreasing the solution flow rate can improve the performance of ED for liquid desiccant regeneration.

Fig. 7 shows the simulated concentration profiles of LiCl solution at the inlet and outlet of the ED cells under different solution flow rates (60, 100 and 140 L/h) and the applied current of 8 A and the concentrations of both spent and regenerated solutions at the ED inlet of 29.031% (wt/wt). In the regenerated channel, the con-

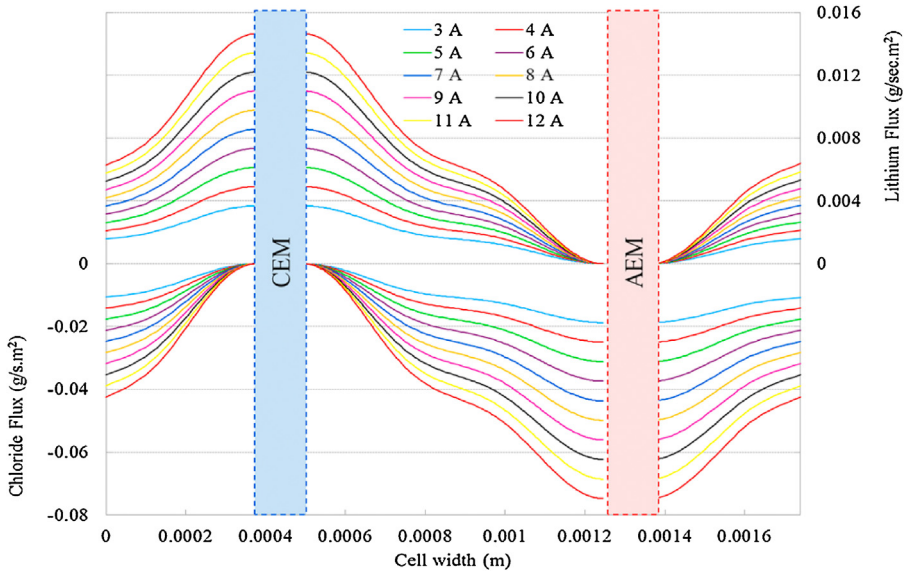

Fig. 9. Profiles of Li^+ and Cl^- fluxes along CEM and AEM under different applied currents.

centration of the bulk solution was always lower than that at the membrane walls, while the concentration of the bulk solution in the spent channels was higher than that at the membrane walls (Fig. 7).

Fig. 7a shows a thin boundary layer at the ED inlet while the thickness of this boundary layer increased gradually along the membrane walls in the regenerated side of the ED channels. A significant boundary layer can be observed at the outlet of the ED cell and the thickness of the boundary layer increased when decreasing the solution flow rate from 140 to 100 and 60 L/h, as shown in Fig. 7b–d.

Fig. 8 illustrates the concentration polarization profile along the length of the CEM and AEM when the concentrations of the solutions at the inlet of both spent and regenerated channels were 29.031% (wt/wt), and the solution flow rate was 60 L/h. The thickness of the boundary layers on the CEM was larger than that on the AEM and this was because the mobility of Cl^- ions was larger than that of Li^+ ions (Strathmann, 2004). As a result, in the regenerated channel, the concentration on the AEM surface was less than that on the CEM surface. The concentration at the membrane walls increased with the increase of the applied current. However, in the spent channel, the concentration at the membrane wall decreased with the increase of the applied current. The maximum concentration at the CEM wall in the regenerated channel was about 30.3% (wt/wt), while the minimum concentration at the same membrane wall in the spent channel decreased to 27.7% (wt/wt) when the applied current was 12 A.

4.6. Flux of ions through membranes

Fig. 9 shows a comparison between the fluxes of Li^+ and Cl^- ions in the bulk solution when the current applied varied from 3 to 12 A under the same concentrations of both spent and regenerated solutions at the ED inlet of 29.031% (wt/wt) and the solution flow rate of 60 L/h. The fluxes of Li^+ and Cl^- ions became dominant around the CEM and AEM of the ED cell, respectively. When the applied current was 12 A, the flux of Li^+ ions was 0.0148 g/s m^2 towards the CEM in the boundary layer while the flux of Cl^- ions was 0.073 g/s m^2 towards the AEM in the boundary layer. However, when the applied current was 3 A, the fluxes of Li^+ and Cl^- ions were 0.0038 and 0.018 g/s m^2 towards the CEM and AEM in the boundary layer, respectively.

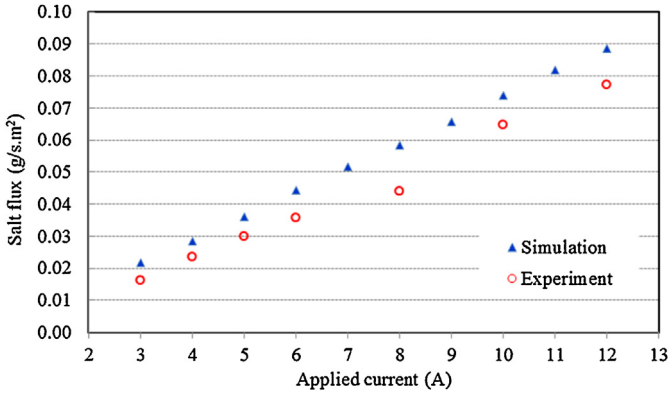

Fig. 10. Comparison of experimentally derived salt flux transferred into the regenerated channels with that determined from simulations.

Fig. 10 presents a comparison between the total salt fluxes migrated into the regenerated channels derived based on the experimental data (i.e. Experimental case 6) and that determined based on the simulation data under different applied currents and the same concentration of both spent and regenerated solutions at the ED inlet of 30% (wt/wt) and the solution flow rate of 100 L/h. It is shown that the total salt flux transferred through the membranes almost linearly increased with the increase of the applied current. The total flux determined from the simulation data generally agreed with that determined from the experimental data.

5. Conclusion

The effects of four key mass transfer mechanisms, namely osmosis, diffusion, electro-osmosis, and ion migration on water and ion transport during the regeneration of LiCl desiccant solution using electrodialysis (ED) were experimentally and numerically investigated. Ion flux, the thickness of the concentration polarization boundary layer, and salt concentration profile along ED membranes were numerically investigated using Nernst-Plank equations, and computational fluid dynamics using COMSOL Multiphysics software. The results showed that water transport due to osmosis is more significant than salt transport. The average water fluxes transferred from the spent to the regenerated solutions within 2 h operation were 0.23 and 0.026 g/s m^2 when the initial concentra-

tion differences between the regenerated and spent solutions were 25 and 5% (wt/wt), respectively. The average salt flux transfer was 0.0053 g/s m^2 when the initial concentration difference between the regenerated and the spent channels was 25% (wt/wt). The flux of water transfer increased with the increase of the applied current but it was decreased with the increase of the solution initial concentration. The average flux of water transfer increased from 0.035 to 0.161 g/s m^2 if the applied current increased from 3 to 12 A under the same initial concentrations of the solutions in both spent and regenerated tanks of 30% (wt/wt) and the solution flow rate of 100 L/h. The results also showed that the applied current is the most influential parameter on the salt flux through the membranes. The salt flux transfer inside the ED stack was in the range of 0.079–0.082 g/s m^2 among the experimental set designed using an orthogonal layout when the applied current was 12 A.

The results also showed that, unlike conventional desalination applications using ED, water transport due to osmosis and electro-osmosis during the regeneration of LiCl liquid desiccant could not be neglected. The experimental results showed that the concentration difference between the regenerated and spent LiCl solutions should be minimized in order to achieve a better ED regeneration performance.

Acknowledgements

The authors would like to thank Mr. Craig McLauchlan and Mr. John Barron for their work to set up the experimental system. Ali Al-Jubainawi would also like to thank the Higher Committee for Educational Development (HCED) in Iraq for the PhD sponsorship support.

Appendix A. Dimensions of the ED model and experimental setup.

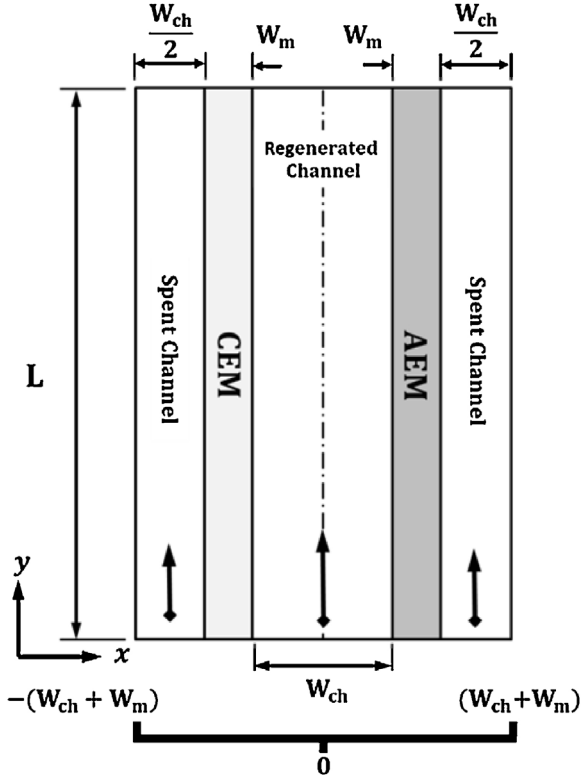

Fig. A1. Illustration of the ED model and its dimensions.

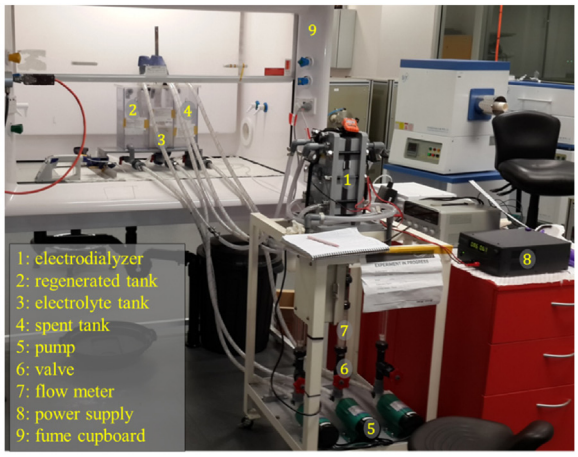

(a) Lab-scale experimental setup

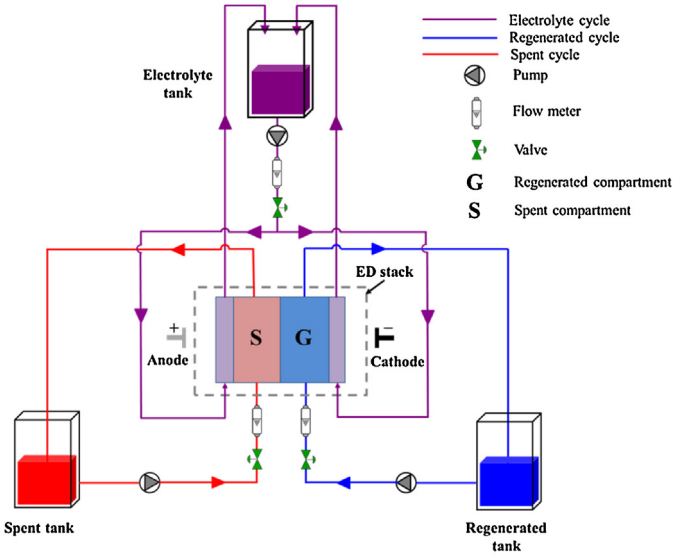

(b) Schematic of the ED operation

Fig. A2. Illustration of the ED experimental setup used for liquid desiccant regeneration. (a) Lab-scale experimental setup, (b) Schematic of the ED operation.

Appendix B. Main characteristics of the ED and measuring instruments used.

Table B1
Main characteristics of the ED experimental setup and inputs of the ED model.

Items	Value	Source
Storage capacity of spent, regenerated and electrolyte tanks	3.5 L	Selemion (2014)
Effective area of the membrane (m^2)	0.021	Selemion (2014)
Number of cells of ED	10	Selemion (2014)
Total potential drop over unit cell (volt)	1.4	
Diffusion coefficient, Li^+ (m^2/s)	2.31×10^{-9}	Strathmann (2004)
Diffusion coefficient, Cl^- (m^2/s)	3.11×10^{-9}	Strathmann (2004)
Temperature (K)	298.15	
Inlet concentration of regenerated and spent solutions (% (wt/wt))	29.031	
Membrane charge concentration, Li^+ (% (wt/wt))	4	Tanaka (2010)
Membrane charge concentration, Cl^- (% (wt/wt))	10	Tanaka (2010)
CMV membrane conductivity (S/m)	0.625	Tanaka (2010)
AMV membrane conductivity (S/m)	0.35	Tanaka (2010)
Channel average flow rate (L/h)	60	–
Cell length, L (m)	0.175	Selemion (2014)
Channel width, W_{ch} (mm)	0.75	Selemion (2014)
Membrane thickness, W_m (mm)	0.12	Selemion (2014)
ED cell depth (m)	0.12	Selemion (2014)
Transport number of water due to electro-osmotic influence (−)	1.2	Experimentally determined
Membrane water permeability due to osmotic pressure per cell ($mol/m^2.s.bar$)	1.147×10^{-5}	Experimentally determined

Table B2
Measuring instruments and measurement accuracies.

Name	Mode	Measurement range	Accuracy
Rectifier	PowerTech MP3090	40 A/15 V DC	±1.0%
Density meter and temperature measurement	30PX Densito	2.0000 g/cm3	±0.001 g/cm3
		40.0 °C	±0.2 °C
Flow meter	TOKYO KEISO AC-1510-4/6	600 L/h	±3% F.S.
Volumetric tanks	–	3.5 L	±0.01 L

References

Al-Sulaiman, F. A., Gandhidasan, P., & Zubair, S. M. (2007). Liquid desiccant based two-stage evaporative cooling system using reverse osmosis (RO) process for regeneration. *Applied Thermal Engineering*, *27*(14), 2449–2454.

Amjad, Z. (1993). *Reverse osmosis: Membrane technology, water chemistry & industrial applications*. New York: Van Nostrand Reinhold.

Bawornruttanaboonya, K., Devahastin, S., Yoovidhya, T., & Chindapan, N. (2015). Mathematical modeling of transport phenomena and quality changes of fish sauce undergoing electrodialysis desalination. *Journal of Food Engineering*, *159*, 76–85.

Casas, S., Bonet, N., Aladjem, C., Cortina, J., Larrotcha, E., & Cremades, L. (2011). Modelling sodium chloride concentration from seawater reverse osmosis brine by electrodialysis: Preliminary results. *Solvent Extraction and Ion Exchange*, *29*(3), 488–508.

Casas, S., Aladjem, C., Cortina, J., Larrotcha, E., & Cremades, L. (2012). Seawater reverse osmosis brines as a new salt source for the chlor-alkali industry: Integration of NaCl concentration by electrodialysis. *Solvent Extraction and Ion Exchange*, *30*(4), 322–332.

Cheng, Q., Xu, Y., & Zhang, X.-S. (2013). Experimental investigation of an electrodialysis regenerator for liquid desiccant. *Energy and Buildings*, *67*, 419–425.

Cheng, Q., Zhang, X. S., & Li, X. W. (2013). Performance analysis of a new desiccant pre-treatment electrodialysis regeneration system for liquid desiccant. *Energy and Buildings*, *66*, 1–15.

Chua, K., Chou, S., Yang, W., & Yan, J. (2013). Achieving better energy-efficient air conditioning – a review of technologies and strategies. *Applied Energy*, *104*, 87–104.

Daou, K., Wang, R., & Xia, Z. (2006). Desiccant cooling air conditioning: A review. *Renewable and Sustainable Energy Reviews*, *10*(2), 55–77.

Dickinson, E. J., Ekström, H., & Fontes, E. (2014). COMSOL Multiphysics®: Finite element software for electrochemical analysis. A mini-review. *Electrochemistry Communications*, *40*, 71–74.

Duan, Z., Zhan, C., Zhang, X., Mustafa, M., Zhao, X., Alimohammadisagvand, B., et al. (2012). Indirect evaporative cooling: Past, present and future potentials. *Renewable and Sustainable Energy Reviews*, *16*(9), 6823–6850.

Fadaei, F., Shirazian, S., & Ashrafizadeh, S. N. (2011). Mass transfer modeling of ion transport through nanoporous media. *Desalination*, *281*, 325–333.

Fidaleo, M., & Moresi, M. (2005). Optimal strategy to model the electrodialytic recovery of a strong electrolyte. *Journal of Membrane Science*, *260*(1), 90–111.

Guo, Y., Ma, Z., Al-Jubainawi, A., Cooper, P., & Nghiem, L. D. (2016). Using electrodialysis for regeneration of aqueous lithium chloride solution in liquid desiccant air conditioning systems. *Energy and Buildings*, *116*, 285–295.

Holloway, R. W., Childress, A. E., Dennett, K. E., & Cath, T. Y. (2007). Forward osmosis for concentration of anaerobic digester centrate. *Water Research*, *41*(17), 4005–4014.

Kim, Y. (2010). *Ionic separation in electrodialysis: Analyses of boundary layer, cationic partitioning, and overlimiting current (Doctor of Philosophy)*. University of Texas at Austin. Retrieved from. https://repositories.lib.utexas.edu/handle/2152/ETD-UT-2010-08-1724

Li, X. W., & Zhang, X. S. (2009). Photovoltaic-electrodialysis regeneration method for liquid desiccant cooling system. *Solar Energy*, *83*(12), 2195–2204.

Li, X. W., Zhang, X. S., & Quan, S. (2011). Single-stage and double-stage photovoltaic driven regeneration for liquid desiccant cooling system. *Applied Energy*, *88*(12), 4908–4917.

Lin, W., Ma, Z., Sohel, M. I., & Cooper, P. (2014). Development and evaluation of a ceiling ventilation system enhanced by solar photovoltaic thermal collectors and phase change materials. *Energy Conversion and Management*, *88*, 218–230.

Marszal, A. J., Heiselberg, P., Bourrelle, J., Musall, E., Voss, K., Sartori, I., et al. (2011). Zero Energy Building – A review of definitions and calculation methodologies. *Energy and Buildings*, *43*(4), 971–979.

Misha, S., Mat, S., Ruslan, M., & Sopian, K. (2012). Review of solid/liquid desiccant in the drying applications and its regeneration methods. *Renewable and Sustainable Energy Reviews*, *16*(7), 4686–4707.

Mohammad, A. T., Mat, S. B., Sulaiman, M., Sopian, K., & Al-abidi, A. A. (2013). Historical review of liquid desiccant evaporation cooling technology. *Energy and Buildings*, *67*, 22–33.

Nikonenko, V., Lebedev, K., Manzanares, J., & Pourcelly, G. (2003). Modelling the transport of carbonic acid anions through anion-exchange membranes. *Electrochimica Acta*, *48*(24), 3639–3650.

Niu, X., Xiao, F., & Ma, Z. (2012). Investigation on capacity matching in liquid desiccant and heat pump hybrid air-conditioning systems. *International Journal of Refrigeration*, *35*(1), 160–170.

Ortiz, J., Sotoca, J., Exposito, E., Gallud, F., Garcia-Garcia, V., Montiel, V., et al. (2005). Brackish water desalination by electrodialysis: Batch recirculation operation modeling. *Journal of Membrane Science*, *252*(1), 65–75.

Pérez-Lombard, L., Ortiz, J., & Pout, C. (2008). A review on buildings energy consumption information. *Energy and Buildings*, *40*(3), 394–398.

Sadrzadeh, M., Kaviani, A., & Mohammadi, T. (2007). Mathematical modeling of desalination by electrodialysis. *Desalination*, *206*(1), 538–546.

Selemion, A. (2014). Retrieved from http://www.selemion.com/SELC.pdf, Access16/3/2014.

Strathmann, H. (2004). *Ion-exchange membrane separation processes*. Amsterdam: Elsevier.

Tanaka, Y. (2003). Mass transport and energy consumption in ion-exchange membrane electrodialysis of seawater. *Journal of Membrane Science*, *215*(1), 265–279.

Tanaka, Y. (2006). Irreversible thermodynamics and overall mass transport in ion-exchange membrane electrodialysis. *Journal of Membrane Science*, *281*(1), 517–531.

Tanaka, Y. (2010). *Ion exchange membrane electrodialysis: Fundamentals, desalination, separation*. New York: Nova Science Publishers.

Wang, S., Ma, Z., & Gao, D. C. (2010). Performance enhancement of a complex chilled water system using a check valve: Experimental validation. *Applied Thermal Engineering*, *30*(17), 2827–2832.
Wang, M., Xing, H. B., Jia, Y. X., & Ren, Q. C. (2015). A zero-liquid-discharge scheme for vanadium extraction process by electrodialysis-based technology. *Journal of Hazardous Materials*, *300*, 322–328.
Waugaman, D., Kini, A., & Kettleborough, C. (1993). A review of desiccant cooling systems. *Journal of Energy Resources Technology*, *115*(1), 1–8.
Yang, W., Sun, L., & Chen, Y. (2015). Experimental investigations of the performance of a solar-ground source heat pump system operated in heating modes. *Energy and Buildings*, *89*, 97–111.
Zhao, S., & Zou, L. (2011). Effects of working temperature on separation performance, membrane scaling and cleaning in forward osmosis desalination. *Desalination*, *278*(1), 157–164.
Zourmand, Z., Faridirad, F., Kasiri, N., & Mohammadi, T. (2015). Mass transfer modeling of desalination through an electrodialysis cell. *Desalination*, *359*, 41–51.